

# Dead Sea Mud Slurry Flow in a Horizontal Pipe

Abdelaziz Khlaifat\*, Taha Al-Khamis

Department of Chemical Engineering, Mutah University, Mutah 61710, Jordan

## Abstract

This paper reports the results of experimental work on the flow of Dead Sea mud through a circular pipe. The dependence of the discharge of the Dead Sea mud in pipe on water content is examined for four different mud-water mixtures that were pumped through a horizontal pipe. A mathematical model describing all observed phenomena was developed. Experimental results were compared with prediction, using shear stress power law equation, and good agreement was obtained. The obtained results may find their application not only in the transportation of Dead Sea mud, but also in assessing the pumping requirements for the transportation of dredged cohesive mud at in-situ water content.

© 2009 Jordan Journal of Mechanical and Industrial Engineering. All rights reserved

Keywords: Flow; Mud; Dead Sea; Slurry; Non-Newtonian.

## Nomenclature

k	flow consistency index
L	pipe length
n	flow behavior index
P	pressure
Q	volumetric flow rate
r	radial direction (m)
R	pipe radius (m)
$\mathcal{U}$	slurry velocity (m/s)
Z	axial direction (m)

## Greek letters

$\mu$	viscosity (N.s/m <sup>2</sup> )
$\tau$	shear stress
$\theta$	angular direction

## Subscripts

z	axial direction
app	apparent
inlet	
L	outlet
rz	in z-direction on a unit area perpendicular to the r-direction.

## 1. Introduction

One of the most raved-about muds in the world comes from the Dead Sea in Jordan. Detailed information about the Dead Sea and the effect of brine evaporation on its content were discussed in [1]. Dead Sea black mud (because of its color) is a mixture of Dead Sea minerals and organic materials naturally formed over thousands of

years on the bed of the Dead Sea. Physical properties, chemical, and mineralogical compositions of the Dead Sea mud were investigated for three different locations on the Eastern shore of the Dead Sea [2]. Due to its mineralogical contents, Dead Sea black mud replenishes the skin minerals essential for renewal and regeneration by removing toxins and dead cells with an exfoliating action. Its cleans, purifies, and rejuvenates skin tissue giving a brighter complexion [3-4]. Black Mud also stimulates blood and lymph circulation, increasing Oxygen intake and draining trapped fluids. It is therefore effective in treating cellulite and in alleviating arthritic and rheumatic conditions [5-6]

Different skin care products, bath salts, and cosmetics products are manufactured from the Dead Sea black mud. Large amount of this mud has to be collected, using special scoops, from different locations on the shore of the Dead Sea, then transported by trucks to the company site where the mud is pretreated and packed in small portions, then shipped to different manufacturers.

In this manuscript, we suggest hydraulic transportation of Dead Sea mud instead of dealing with the mentioned-above tedious process of mud collection and handling. Hydraulic transportation of Dead Sea mud in a circular pipe requires mixing the mud with water to decrease the mud viscosity, and accordingly friction. In order to minimize the mud pretreatment cost, industries which will pump Dead Sea mud will be under continuous pressure to decrease water content and increase mud concentration. At high concentration, the viscous forces, which are usually highly non-Newtonian and yield stress in nature, become dominant, and mud flows inevitably becomes laminar [7]. The objective of this paper is to demonstrate that the Dead Sea mud can be pumped from its source to the exploiting industry and to show and evaluate the impact of changing

\* Corresponding author. khlaifat@mutah.edu.jo.

non-Newtonian viscous stresses have on pipelining problem.

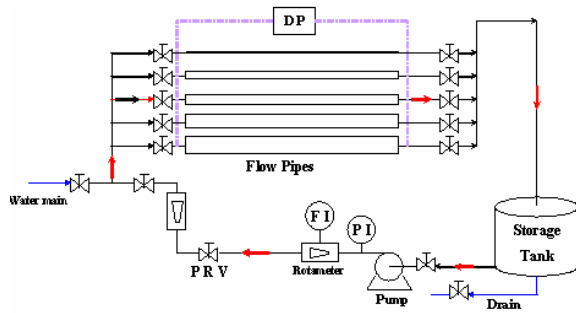


Figure 1. Experimental Setup.

## 2. Experimental Setup

One of the problems that are facing the industrial companies that deal with the Dead Sea Mud is the mud transport. Unlike pure water transport, mud transport is very complicated and expensive because of both its composition and high viscosity. High mud viscosity results in a very high shear stress while flowing. The high shear stress can be overcome only by having a very high pressure drop that needs to be generated by special pumps.

As it can be seen from Figure 1, the experimental setup consists of five-pipes network consisting of ¼ inch, nominal size pipe branch, a ½ inch branch, a ¾ inch branch, a 1 inch, and 2 inch branch all galvanized, schedule 40 were assembled. The setup can operate as closed or open loop system. The closed loop system consists of a storage tank, a pump, a pressure regulator, two rotameters (low and high range), and a differential pressure gauges (DP). Only the pipe with an inside diameter ½" and length 2m was used in this study and the system operated as closed loop, which consists of a storage tank, a pump, four valves and a manometer to measure the pressure drop. Distilled water was added to the Dead Sea Mud to prepare slurries with four different concentrations.

## 3. Mathematical Model

Flow of fluids in circular tubes is encountered to be the more economical and rapid transportation method than others, such as those involving conveyor systems. The mathematical model that describes the mud flow inside a pipe is developed based on the basic principles of continuity and momentum equations. The z-component of the Navier-Stokes momentum equation is simplified for steady state, laminar, incompressible and isothermal mud slurry flow in a horizontal pipe, as shown in Fig 1. It was postulated that the only non-vanishing velocity component is the axial velocity ( $v_z$ ). The axial velocity, for fully developed flow, is a function of radial direction. Simplification of the z-component of momentum equation yields an expression for shear stress as follows:

$$\tau_{rz} = \frac{P_L - P_0}{2L} r \quad (1)$$

Where  $P_L$  is the outlet pressure (at  $z = L$ );  $P_0$  is the inlet pressure (at  $z = 0$ );  $L$  is the pipe length; and  $r$  is

the radial direction. The non-Newtonian power law of viscosity, [9], is used for the Dead Sea mud slurry as:

$$\tau_{rz} = -k \left( -\frac{dv_z}{dr} \right)^n \quad (2)$$

Where:  $k$  is the flow consistency index and  $n$  is the flow behavior index. Inserting Eq. (2) into Eq. (1), rearrange and integrate, then apply the no-slip condition at the wall ( $v_z(r = R) = 0$ ) to determine the integration constant. The final velocity profile expression will be:

$$v_z = \left( \frac{P_L - P_0}{2Lk} \right)^{\frac{1}{n}} \left( \frac{n}{n+1} \right) R^{\frac{n+1}{n}} \left[ 1 - \left( \frac{r}{R} \right)^{\frac{n+1}{n}} \right] \quad (3)$$

The velocity profile in Eq. (3) can be used to calculate:

1- The slurry maximum velocity ( $v_{z,max}$ ):

The maximum velocity occurs at the centerline ( $r = 0$ ) and has the value

$$v_{z,max} = \left( \frac{P_L - P_0}{2Lk} \right)^{\frac{1}{n}} \left( \frac{n}{n+1} \right) R^{\frac{n+1}{n}} \quad (4)$$

2- The slurry average velocity ( $v_{z,average}$ ):

The average velocity is obtained by dividing the total volumetric flow rate by the cross-sectional area:

$$v_{z,average} = \frac{\int_0^{2\pi R} \int_0^{2\pi R} v_z r dr d\theta}{\int_0^{2\pi R} \int_0^{2\pi R} r dr d\theta} = \left( \frac{P_L - P_0}{2Lk} \right)^{\frac{1}{n}} \left( \frac{n}{n+1} \right) R^{\frac{n+1}{n}} \left[ \frac{n+1}{3n+1} \right] \quad (5)$$

3- The slurry volumetric flow rate (Q):

The volume rate of flow is the product of area and average velocity, thus:

$$Q = \int_0^{2\pi R} \int_0^{2\pi R} v_z r dr d\theta = (v_{z,average})(Area) \\ = \left( \frac{P_L - P_0}{2Lk} \right)^{\frac{1}{n}} \left( \frac{n}{n+1} \right) R^{\frac{n+1}{n}} \left[ \frac{n+1}{3n+1} \right] (\pi R^2) \quad (6)$$

Table 1. Dead Sea and distilled water content (Vol. %) in different runs.

Run Number	Distilled Water	Dead Sea Mud
1	10	90
2	15	85
3	20	80
4	25	75

## 4. Results and Discussion

Four experimental runs were carried out based on different Dead Sea mud volume fractions, as shown in Table 1. The slurries were prepared by adding distilled

water with volume fractions of 10%, 15%, 20% and 25%, to the Dead Sea mud volume fractions, shown in Table 1. The obtained suspensions, and before being used, were stirred continuously for 30 minutes.

Several tests of slurry runs were carried out at different pressure drops. Prior to each run, the slurry was mixed as stated above for a time sufficient to achieve homogeneous mixture. For each run, a representative sample of the slurry was collected to measure its density and percentage of solid by weight and volume. The results of these measurements are shown in Tables 2, 3 and 4, respectively.

Table 2. Density of Dead Sea Mud Slurry for Different Mud Concentration.

Experimental Run Number	1	2	3	4
Slurry Averaged Density, $kg/m^3$	1103	1067	1062	1038

Table 3. Percent of solid by weight for different concentrations of the Dead Sea Mud in the slurry

Experimental Run Number	1	2	3	4
Percent of solid by weight	14.53	9.88	8.40	6.99

Table 4. Percent of solid by volume for the slurry with different mud concentrations.

Experimental Run Number	1	2	3	4
Total volume (ml)	390	250	415	236
Volume of solid (ml)	114	61	90	38
Percent of solid by volume %	29.23	24.40	21.69	16.10

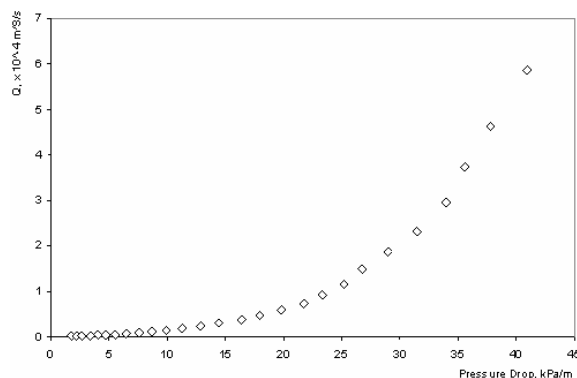


Figure 2. Slurry Volumetric Flow Rate Versus Pressure Drop for the Case of 90% Dead Sea Mud.

Figure 2 shows the operating conditions and measured exit slurry flow rate for the case of 90% Dead Sea mud volume fraction. As Fig. 2 shows, the slurry flow rate has nonlinear relationship with the pressure drop. For small pressure drop, slurry flow rate is almost negligible and changes in linear fashion, and when the pressure drops becomes greater than 10 kPa/m, the deviation from linear behavior starts. The volumetric flow rate versus pressure drop for other slurries with different Dead Sea mud volume fractions are shown in Fig. 3. From this figure, it is obvious that at low pressure drop, 10 kPa/m, there is no

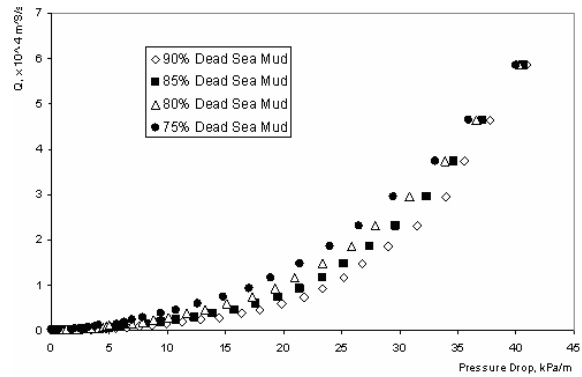


Figure 3. Volumetric Flow Rate Versus Pressure Drop for Slurries with Different Dead Sea Mud Volume Fractions .

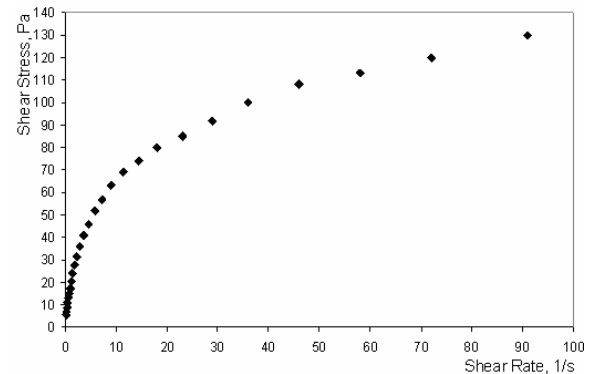


Figure 4. Shear Stress Versus Shear Rate for the Case of 90% Dead Sea Mud.

difference in slurry flow rate at different compositions. Also, at higher pressure drop, 25 kPa/m, the flow rate for the slurry with 75% Dead Sea mud is the highest. This can be explained by the fact that when the volume fraction of distilled water is increased, the slurry density decreases as shown in Table 2, and the slurry tends to behave as a Newtonian fluid where smaller driving force is needed to overcome the resistance to the flow. Also, from Fig 3 one can see that as the Dead Sea mud fraction in the slurry decreases, the volumetric flow rate – pressure drop curves become less concaved. This is seen very clear for the highest water volume fraction in the slurry (25%).

For unidirectional, laminar and steady flow in a circular pipe, the shear stress  $\tau_w$ , in Pa, at the inside wall of the pipe can be calculated by  $\tau_w = (D/4)(\Delta P/L)$  [8,9, and 10], where D is the pipe inside diameter, and  $\Delta P/L$  is the pressure drop in Pa/m. The shear stress rate for the flow in the pipe can be calculated as  $32Q/\pi D^3$  [10-11], and has a unit (1/s). Fig. 4 presents the experimental data for shear stress at the pipe inside wall versus the mean shear rate for slurry with 90% Dead Sea mud volume fraction. The nonlinear relationship between shear stress and shear rate attests the fact that the used slurry is not Newtonian fluid. Figure 5 shows a comparison between steady state slurry shear stress results for four different slurry compositions (90%, 85%, 80%, and 75% Dead Sea mud volume fractions). From this figure, one can see that the shear stress and shear rate curve for the case of slurry with 90% Dead Sea mud is the highest, while the curve for the slurry with lowest Dead Sea mud content is the lowest. This could be explained by the fact that as more water is added to the slurry, it gets thinner and behaves closer to Newtonian fluid. If large amount of water is added to the

slurry, it is expected that the relationship between shear stress and shear rate, Fig 5, will become linear.

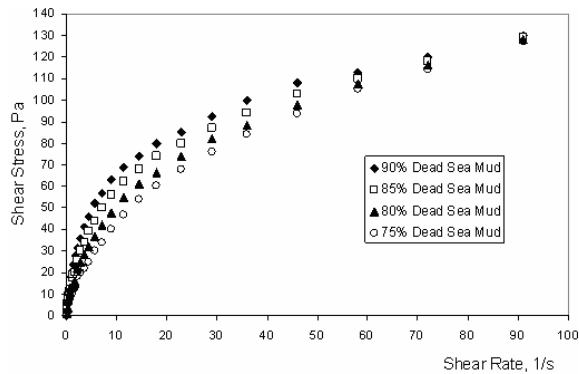


Figure 5. Shear Stress Versus Shear Rate for Slurries with Different Dead Sea Mud Volume Fractions.

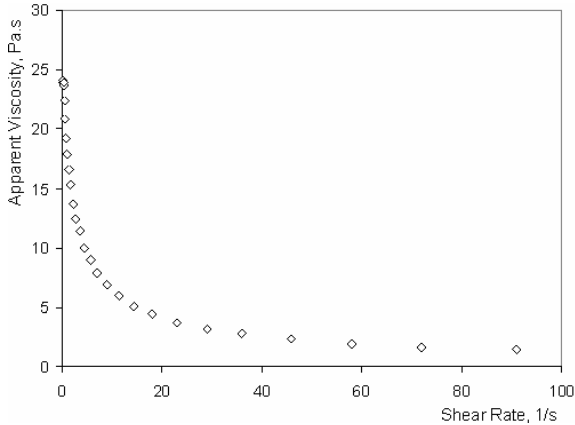


Figure 6. Apparent Viscosity Versus Shear Rate for the Slurry with 90% Dead Sea Mud.

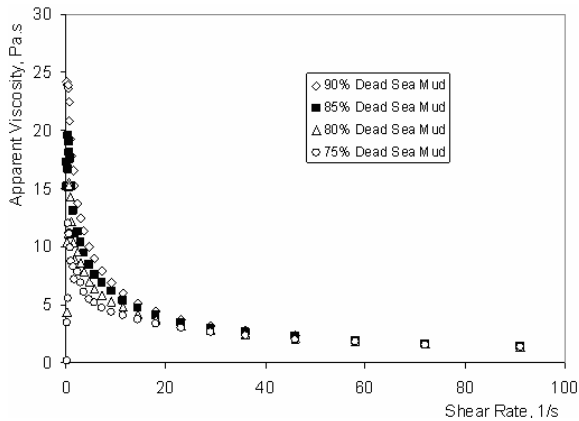


Figure 7. Apparent Viscosity Versus Shear Rate for Slurries with Different Dead Sea Mud Volume Fractions.

From Figures 4 and 5 at low values of flow rates (mean velocities), the profiles are almost linear. Because of the large densities of the slurries (Table 2) in comparison with Newtonian fluid, the straight lines pass through the origin and closer to the shear stress axis. All the trends between shear stress and shear rate attest to the validity of the power law assumption, Eq. (2), made for shear stress.

In order to check whether the obtained results are in good agreement with predictions (power law), the viscosity was expressed as an apparent viscosity. The apparent viscosity,  $\mu_{app}$ , was calculated at each data point as the shear stress divided by the shear rate. The slurry

composites are restated here, using apparent viscosity versus shear rate as shown in Figure 6. It can be seen from this figure that the viscosity profile shows an exponential decrease as a function of shear rate. Similar trends were observed for slurry with other composition (Figure 7). From Fig., 7 it is obvious that the thinned with increasing shear rate. To understand the exponential decrease behavior between apparent viscosity shear rate, the shear stress power law equation, Eq. (2) is inserted into the apparent viscosity expression to have:

$$\mu_{app} = \frac{\text{shear stress}}{\text{shear rate}} = \frac{\tau_w}{dv_z/dr} = k \left( \frac{dv_z}{dr} \right)^{n-1} \quad (7)$$

Taking the logarithm of both sides of Eq. (7), we obtain:

$$\log(\mu_{app}) = \log(k) + (n - 1) \log \left( \left| \frac{dv_z}{dr} \right| \right) \quad (8)$$

Figure 8 shows the observed behavior between apparent viscosity and shear rate (plotted on a log-log scale for 90% Dead Sea mud slurry). From Equation (8) and when  $n = 1$ , zero slope in equation (8), the slurry behaves as a Newtonian fluid. This behavior is observed in Fig 8 for small shear rate (less than 0.55/s) where the viscosity of the slurry is about 23.89 Pa.s. Linear regression for high shear rate (from 9 to 100  $S^{-1}$ ) gives a negative slope with a value of (-0.6894) from which one can determine that  $n = 0.3106$ , and an intercept of 1.5087 ( $\log k = 1.5087$ ) from which one can determine that  $k = 32.2627 \text{ Pa.s}^{0.3106}$ . Because of the fact that the Newtonian fluid behavior region contains few points, the entire region can be fitted using a power law model to have  $n = 0.507$  and  $k = 17.51 \text{ Pa.s}^{0.507}$ . Similar trends were observed for slurries with other compositions (Figure 9). It is clear from this figure that the viscosity is decreasing smoothly for all slurries with increasing shear rate.

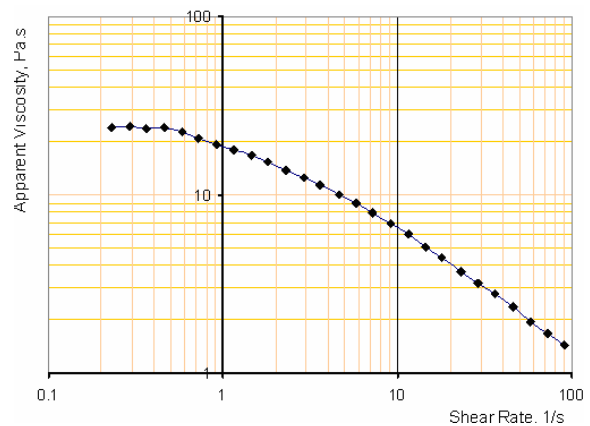


Figure 8. Apparent Viscosity Versus Shear Rate for the Slurry with Dead Sea Mud Volume Fraction of 90%.

Consistency index (k) and flow index (n) in equation (8) were calculated using power regression analysis of the data for apparent viscosity versus shear rate. The results of these calculations at different slurry compositions are tabulated in Table 5 for three cases: a) using all data; b) excluding the data points that result in some scatter of the

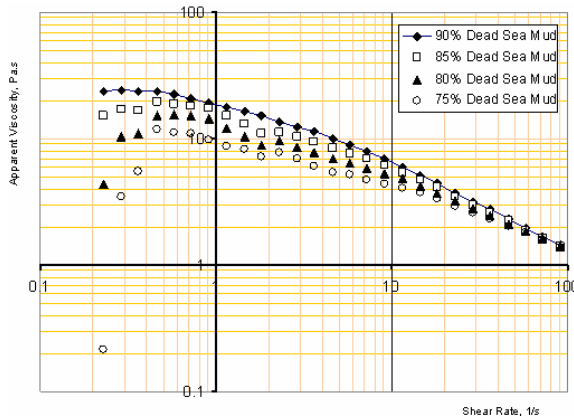


Figure 9. Apparent Viscosity Versus Shear Rate for Slurries with Different Dead Sea Mud Volume Fractions.

Table 5. Comparison Between Calculated Consistency and Flow Indices for Slurries with Different Dead Sea Mud Compositions.

Case	Run 1		Run 2		Run 3		Run 4	
	n	k, Pa.s <sup>n</sup>	n	k, Pa.s <sup>n</sup>	n	k, Pa.s <sup>n</sup>	n	k, Pa.s <sup>n</sup>
a	0.507	17.51	0.5571	13.92	0.6452	9.91	0.8301	5.36
b	0.4479	20.54	0.4855	16.88	0.5289	13.52	0.5955	9.96
c	0.3106	32.26	0.3553	26.12	0.4162	19.83	0.4901	14.29

viscosity at lower shear rate; and c) using the data points at high shear rate that result in linear relationship between apparent viscosity and shear rate. From this table, the calculated flow index is always less than one which means that the slurry is shear thinning. The more shear-thinning the slurry, the greater the friction reduction is. Also, Table 5 shows that when the water content is increased in the slurry, the flow index (n) increases for the above-mentioned three cases. Because flow index, in essence, is a measure of non-Newtonian-ness and for a Newtonian fluid  $n = 1$ ; the increase in the flow index makes the slurry to behave as close as possible to the Newtonian fluid. Table 5 shows that for the three considered cases, we have a viscosity decrease with increasing flow behavior index; this behavior is very consistent with the slurry tendency to behave as Newtonian fluid.

**5. Conclusions**

Although the behavior of mud flow is complex and the theory of its behavior is not well developed, simplifying assumptions were made to permit an analytical solution

and provide insight into the influence of various parameters on the results of the laboratory tests.

This paper highlights the importance of a thorough rheological analysis of non-Newtonian fluids such as Dead Sea mud slurry. Power law was used to accurately represent the interaction between shear stress and viscosity and velocity gradient. Apparent viscosity – shear rate relation exhibits very valuable profiles to determine both flow consistency index and flow behavior index. The developed mathematical model could predict the flow rate of Dead Sea mud slurry through a pipe under the conditions of applied pressure drop. Experimental work showed that the slurry with low Dead Sea mud content behaves closer to Newtonian fluid.

**References**

- [1] A. Al-Khlaifat, “Dead sea rate of evaporation”. American Journal of Applied Sciences, Vol. 5, No. 8, 2008, 934-942.
- [2] A. Khlaifat, O. Khashman, “Physical and chemical characterization of Dead Sea mud”. submitted for possible publication to Journal of Materials Characterization.
- [3] R. Schiffner, J. Schiffner-Rohe, M. Gerstenhauer, M. Landthaler, F. Hofst dter, W. Stolz, “Dead Sea treatment - principle for outpatient use in atopic dermatitis: safety and efficacy of synchronous balneophototherapy using narrowband UVB and bathing in Dead Sea salt solution”. Euro J Dermatol, Vol. 12, No. 6, 2002, 543-548.
- [4] S. Halevy, S Sukenik, “Different modalities of spa therapy for skin diseases at the Dead Sea area”. Arch Dermatol, Vol. 134, No. 11, 1998, 1416-1420.
- [5] S. Bellometti, M. Poletto, C. Gregotti, P. Richelmi, F. Berte, “Mud bath therapy influences nitric oxide, myeloperoxidase and glutathione peroxidase serum levels in arthritic patients”. Int J Clin Pharmacol Res, Vol. 20, No. 3, 2000, 69-80.
- [6] S. Sukenik, D. Buskila, L. Neumann, A. Kleiner-Baumgarten, “Mud pack therapy in rheumatoid arthritis”. Clin Rheumatol, Vol 11, No. 2, 1992, 243-247.
- [7] R. Haldenwang, P. T. Slatter, S. Vanyaza, R. P. Chhabra, “The effect of shape on laminar flow in open channels for non-Newtonian fluids”. J Hydrotransport, Vol 16, 2004, 311-324.
- [8] Bird R B, Stewart W E, Lightfoot E N. Transport phenomena. 2<sup>nd</sup> ed. New York; John Wiley & Sons; 2002.
- [9] Noel de Nevers. Fluid mechanics for chemical engineers. 2<sup>nd</sup> ed. McGraw-Hill; 1991.
- [10] Wilkes J O. Fluid mechanics for chemical engineers. Prentice Hall; 1999.
- [11] J. Billingham, J. Ferguson, “Laminar unidirectional flow of a thixotropic fluid in a circular pipe”. J. Non Newtonian Fluid Mech, Vol. 47, 1993, 21-55.

